Pis'ma v ZhETF, vol. 102, iss. 5, pp. 322 – 326

Phase transition for edge band emergence induced by edge relaxation of phosphorene ribbons

M. Yang[1)], *H.-J. Duan, R.-Q. Wang*

Guangdong Provincial Key Laboratory of Quantum Engineering and Quantum Materials, School of Physics and Telecommunication Engineering, South China Normal University, 510006 Guangzhou, China

Submitted 23 June 2015

We investigate the edge bands of the relaxed phosphorene edges. The edge relaxation is modeled by letting the outmost bonds be different. By treating the relaxed hopping energy as a parameter, we observe the phase transition for the edge band appearance in the bulk gap. The analytical expression of the relaxed hopping for the phase transition is obtained by means of tight-binding parameters.

DOI: 10.7868/S0370274X15170075

I. Introduction. Mono-layer materials have drawn much attention since graphene was discovered in laboratory [1]. Several alternatives, such as silicene, and metal dichalcogenides exist stably but have their limitations. Graphene has no energy gap [2], carrier mobility of metal dichalcogenides is not high enough [3], and silicene can only be synthesized on metal surfaces [4]. Recently, a new candidate, phosphorene (a monolayer of back phosphorus), was exfoliated from its bulk counterpart, which overcomes all these shortages and shows great potential for application [5].

Phosphorene can be prevent to degrade and can keep high electric quality for long time [6, 7]. Phosphorene field-effect transistors have large on-off current ratio [5], and perform reliably at room temperatures [8]. Phosphorene has a puckered lattice structure, and the projection of it on the layer plane can be viewed as a deformed honeycomb lattice, as shown in Fig. 1a. Due to the lattice puckering, the electronic structure, as well as the collective excitations, exhibit strong anisotropy while the in-plane static screening remains almost isotropic [9, 10]. Phosphorene nanoribbons could be jointed to construct nanotubes without strain energy penalty [11]. It was found that phosphorene sheet can sustain tensile strain up to about 30 % [12] which makes it possible to dramatically modify the properties of phosphorene by applying large strain. It was reported that the energy gap can be adjusted by strain and a semiconductor–metal transition could be induced [13]. The optical response is also anisotropic [14] and sensitive to the orientation of the strain applied [15]. Recently, tight-binding parameters were extracted from ab initio calculations

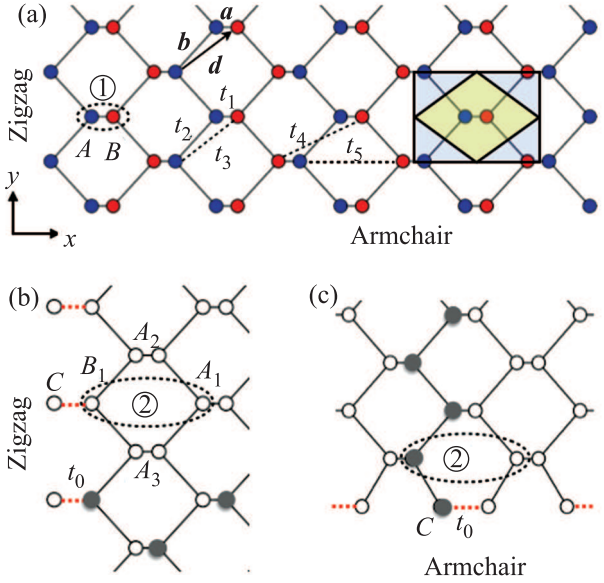

Fig. 1. (Color Online) (a) – Sketch of phosphorene lattice. Red- and blue-filled circles represent puckered up and puckered down atoms, the rectangular shows the primitive cell, and the rhombus illustrates the primitive cell regardless of the puckering. (b, c) – Site and bond configurations of relaxed edges, and the wavefunctions on series of filled sites will be investigated

[16], which provides a platform for further theoretical researches.

It was convinced that there exist edge bands localized near zigzag edges of pristine phosphorene ribbons [17, 18]. The edge bands have their topological origin, which was confirmed by observing the edge band evolution when continuously deforming the standard honeycomb lattice to the phosphorene one [18]. Realistic phosphorene edges are more complicated because of edge re-

[1)]e-mail: yang.mou@hotmail.com

laxation and chemical species termination. Edge states at zigzag edge can be removed by edge hydrogenation [19–22], and also by other species termination on edges [23]. Edge relaxation of the armchair edge results in Peierls transition of the edge atoms (edge atoms get closer pair by pair), which induces few edge bands, but the ribbon remain a semiconductor [22, 24]. These studies on the complex edges are mainly numerical, and analytical models are needed to get some insights on the edge bands of phosphorene ribbons.

In this paper, we investigate the edge bands of the relaxed phosphorene edges. Edge relaxation leads to the bond lengths near edges are different from those in bulk, and thus the hoppings near edges are different. We model the edge relaxation by letting the outmost bonds be different, as shown in Figs. 1b and c. By treating the relaxed hopping energy as a parameter, we observe the phase transition for the edge band appearance in the bulk gap. The analytical expression of hopping energy for the phase transition is obtained. Our calculations could be qualitative explanations for the edge band elimination on hydrogenated zigzag edges, and for the edge band formation on relaxed armchair edges.

II. Tight-binding parameters and bulk Hamiltonian. The energy bands of phosphorene can be well described by the tight-binding model by taking into account five hoppings labeled by t_1 through t_5 shown in Fig. 1a. The values of these hoppings were reported to be (in units of eV) $3.665, -1.22, -0.105, -0.205$, and -0.055, respectively [16]. The nearest hoppings t_1 and t_2 are the largest ones in amplitude, and dominate the basic features of the band structure such as the heavily anisotropy between x- and y-directions. The next-nearest hopping t_3 is quite small, which accounts for the asymmetry between electron and hole dispersions. The next-next-nearest hoppings, t_4 and t_5, result in slight corrections of the anisotropy. The non-nearest parameter t_3, t_4 and t_5 do affect the band structures, but the topological properties of the band structure is dominated by the nearest hoppings [18]. Therefore, we only take the nearest hoppings in to account in this paper.

Due to the atom puckering, one primitive cell of phosphorene lattice is a rectangular containing four atoms. However, the puckering can be ignored after the tight-binding hoppings are obtained (the puckering is already reflected by the relative amplitudes between these hoppings), the lattice was equivalent to its projection on the layer plane, and the primitive cell is reduced to a rhombus which only includes two atoms, as argued in Ref. [18]. The two primitive cells are illustrated in Fig. 1a. The projected phosphorene lattice, like the standard honeycomb lattice, consists of two sublattices named by A and B. In the frame of nearest tight-binding, by selecting a dimer, saying, dimer 1 in Fig. 1a, to study, the bulk Hamiltonian in k-space in basis of A–B sublattices can be immediately written down as

$$H_{\text{bulk}} = \begin{bmatrix} 0 & h \\ h^* & 0 \end{bmatrix}, \qquad h = t_1 + 2t_2 e^{-ik_x d_x} \cos k_y d_y, \tag{1}$$

where $d_x = a + b_x$ and $d_y = b_y$, with a and b being the in-plane bond lengths shown in Fig. 1a, and the subscripts denoting the x- and y-components. The explicit form of h depends on the dimer selection, and any form of h results in the same energy dispersion

$$E^2 = t_1^2 + 4t_1 t_2 \cos k_x d_x \cos k_y d_y + 4t_2^2 \cos^2 k_y d_y. \tag{2}$$

The band edges (bottom of electron band and top of hole band) are the energies at $k_x = 0$ and $k_y = 0$, saying,

$$E(k = 0) = \pm(t_1 + 2t_2). \tag{3}$$

The separation between the two energies is the energy gap.

III. Edge bands. Winding number reflects the number of edge band, and can be deduced from the bulk Hamiltonian by choosing a proper dimer. It can be verified that edge bands can be found on the zigzag edge of phosphorene but cannot on armchair and bearded zigzag edges [18]. However, the winding number analysis can only be applied for the system with standard edges. For realistic ribbons, the bonds between the atoms near edges are different from those between bulk ones due to bond relaxation, reconstruction, and atom absorption, and the winding number is not a good quantity to reflect edge band properties anymore. We model the relaxation and reconstruction by letting the outmost hopping t_0 being a changeable parameter. The site and bond configurations of the edge relaxation model are shown in Figs. 1b and c. In the following, we will refer these bonds as relaxed bonds and the outmost sites connected by the relaxed bonds as relaxed sites. When $t_0 = t_1$, the edge in Fig. 1b is the bearded zigzag and in Fig. 1c is armchair. For the case of $t_0 = 0$, edges in the two figures are zigzag and bearded armchair, respectively.

Fig. 2 shows the evaluation of the band structure of a zigzag ribbon laying along y-direction when the relaxed bond hopping t_0 is tuned from t_1 to 0. When t_0 is deviated from the normal value t_1, a band is gradually peeled from the bulk electron dispersion, and so does another band from the hole dispersion. At a certain value $t_0 = t_C$, the two bands are completely separated

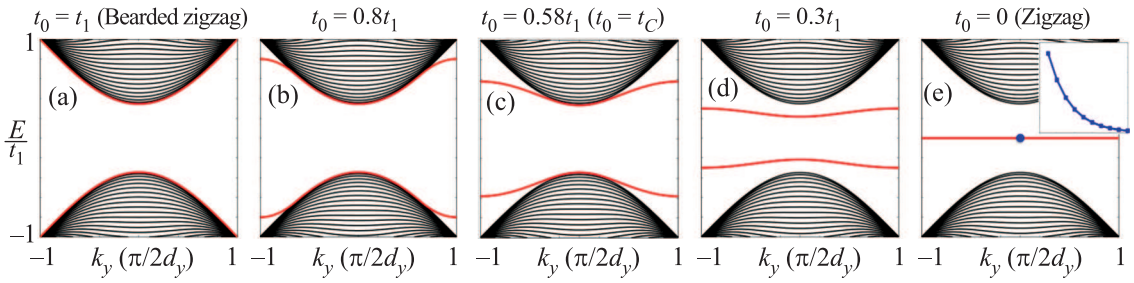

Fig. 2. (Color online) Evalution of band structure of the phosphorene ribbon with the edge shown in Fig. 1b when the relaxed bond t_0 changes from t_1 to 0. The inset illustrates the wavefunction maglitude on those filled sites in Fig. 1b of the state labeled by the dot in e

from the bulk bands, and edge bands appear in the band gap. When t_0 changes on, the edge bands are the more and more apart from the bulk bands and closer to each other. They finally overlap and merge into one flat band when $t_0 = 0$, and the band structure is reduced to the case of zigzag edge. The states of the flat band are edge states, as the inset illustrates.

The properties of band edge can be deduced by solving the effective Hamiltonian of a dimer close to the edge, saying, dimer 2 in Fig. 1b. The effective Hamiltonian consists two parts, a selfenergy $\Sigma_{\rm relax}$ to describe the coupling between dimer 2 and the relaxed site, and $H_{\rm semi}$ to summarize the dimer interacting with other sites exclusive the relaxed site, which is indeed the effective Hamiltonian of the dimer for a semi-infinite system with the relaxed atoms being cut down. We write effective Hamiltonian as

$$H_{\rm dimer2} = H_{\rm semi} + \Sigma_{\rm relax}. \tag{4}$$

The eigen problem of the effective Hamiltonian with combination of Eq. (2) determines all properties of the edge bands. In basis B–A sublattices (we always let the left site of the dimmer be the first), $H_{\rm semi}$ has the form

$$H_{\rm semi} = \begin{bmatrix} 0 & h'_{12} \\ h'_{21} & 0 \end{bmatrix}. \tag{5}$$

The calculation of the elements h'_{12} and h'_{21} relies on the fact that wavefunctions on other sites connecting to dimer 2 can be mapped to the wavefunctions of sites of dimer 2. For instance, site B_1 couples site A_2 and A_3, the wave functions on them are $\psi_{A_2} = e^{-ik_x d_x} e^{ik_y d_y} \psi_{A_1}$ and $\psi_{A_3} = e^{-ik_x d_x} e^{-ik_y d_y} \psi_{A_1}$ and site A_1 is just one site belong to dimer 2 (see Fig. 1b), where k_y is real but k_x is imaginary. By this method, we have the matrix elements

$$\begin{aligned} h'_{12} &= t_2 e^{-ik_x d_x}(e^{ik_y d_y} + e^{-ik_y d_y}), \\ h'_{21} &= t_1 e^{2ik_x d_x} + t_2 e^{ik_x d_x}(e^{ik_y d_y} + e^{-ik_y d_y}). \end{aligned} \tag{6}$$

Dimer 2 coupling to the relaxed site is reflected in the Shrödinger equation of site B_1 by $E\psi_{B_1} = t_0\psi_C + t_2\psi_{A_2} + t_2\psi_{A_3}$, in which $t_0\psi_C$ can be replaced with $t_0^2\psi_{B_1}/E$ by applying the Shrödinger equation of site C, saying, $E\psi_C = t_0\psi_{B_1}$. In matrix language, we have the selfenergy as

$$\Sigma_{\rm relax} = \frac{t_0^2}{E}\begin{bmatrix} 1 & 0 \\ 0 & 0 \end{bmatrix}. \tag{7}$$

Inserting the obtained $\Sigma_{\rm relax}$ and $H_{\rm semi}$ in to Eq. (4), we work out the explicit form of the effective Hamiltonian. The eigen problem of it gives a relation between k_x, k_y and E, which is not enough to obtain the energy dispersions of edge bands, because the imaginary wavevector k_x is not a free variable, but dependent on other quantities, saying, $k_x = k_x(k_y, E)$.

When the phase transition occurs, the wavevector k_x at $k_y = 0$ experiences a change form imaginary number to real one. So we have the constrictions $k_x = 0$ and $k_y = 0$ for the phase transition. Applying the constrictions to Eq. (4), the effective Hamiltonian of dimer 2 is reduced to

$$H_{\rm dimer2} = \begin{bmatrix} t_0/E^2 & 2t_2 \\ t_1 + 2t_2 & 0 \end{bmatrix}. \tag{8}$$

Solving the eigen problem and combining Eq. (3) (the energy for $k_x = 0$ and $k_y = 0$), we immediately have the value of t_0 for the phase transition,

$$t_C = \sqrt{t_1^2 + 2t_1 t_2}. \tag{9}$$

For the adopted hopping parameters, we have $t_C = 0.58t_1$. What happens to the band structure when the phase transition occurs can be seen in Fig. 2c.

Fig. 3 shows the evaluation of the band structure of a armchair ribbon laying along x-direction when the relaxed bond t_0 is changed from t_1 to 0. It tells almost the same story as Fig. 2 does. Edge bands appear gradually

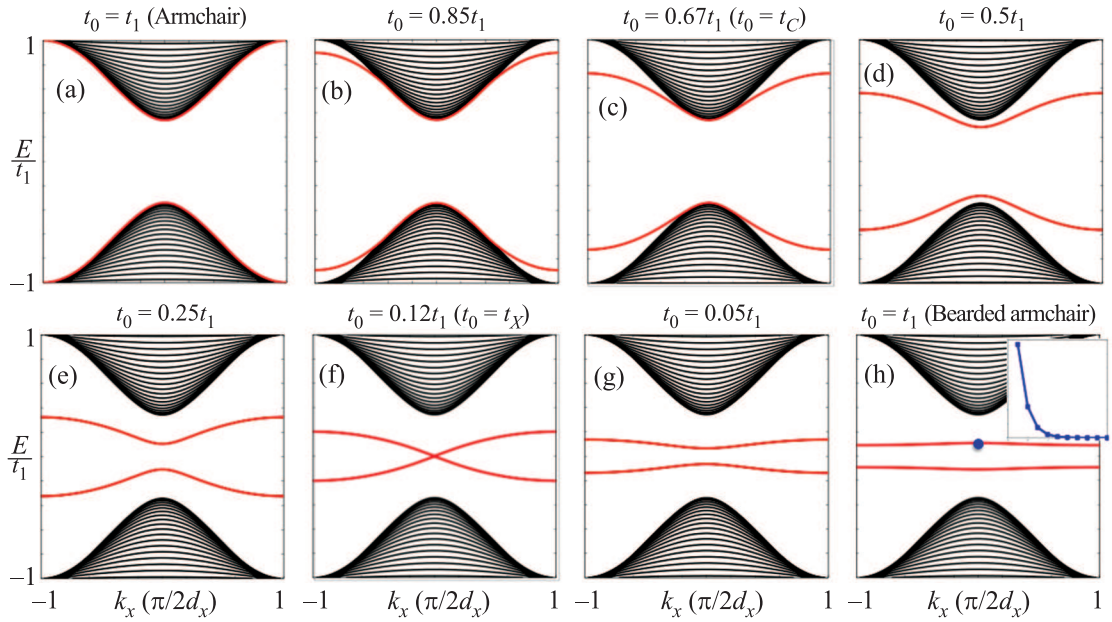

Fig. 3. (Color online) Evalution of band strucuture of the phosphorene ribbon with the edge shown in Fig. 1c when the relaxed bond t_0 changes from t_1 to 0. The inset illustrates the wavefunction maglitude on those filled sites in Fig. 1c of the state labeled by the dot in (h)

when t_0 changes. After t_0 decreases beyond a transition value t_C, the edge bands can be found in the energy gap. Interestingly, at a special value $t_0 = t_X$, a band crossing appears at $k_x = 0$ and a one-dimensional Dirac point arises. When t_0 decreases to 0, the edge bands of bearded armchair ribbon are nearly flat but not zero energy bands. The localization of the edge bands for the bearded armchair edge is illustrated in the inset. The explicit values of t_0 for phase transition and edge band crossing are both determined by the effective Hamiltonian of dimer 2 in Fig. 1c. By the same method we treated the zigzag ribbon, we have the elements of H_{semi},

$$\begin{aligned} h'_{12} &= t_1 e^{-2ik_x d_x} + t_2 e^{-ik_x d_x} e^{ik_y d_y}, \\ h'_{21} &= t_1 e^{2ik_x d_x} + t_2 e^{ik_x d_x} e^{ik_y d_y}. \end{aligned} \tag{10}$$

There are two relaxed sites connected with dimer 2, which causes a little bit more complication than the previous case, but the physics is exactly the same. Without proven, we write down the selfenergy, a k-independent matrix again, as

$$\Sigma_{\text{relax}} = t_2^2 \left[E - t_0 \begin{pmatrix} 0 & 1 \\ 1 & 0 \end{pmatrix} \right]^{-1}. \tag{11}$$

When the phase transition occurs, applying the constrictions $k_x = 0$ and $k_y = 0$ to Eq. (10), we have

$$H_{\text{semi}} = (t_1 + t_2) \begin{bmatrix} 0 & 1 \\ 1 & 0 \end{bmatrix}. \tag{12}$$

Inserting the obtained H_{semi} and Σ_{relax} into Eq. (4), working out the eigen values, and combing Eq. (3), we have the value of t_0 for the phase transition,

$$t_C = t_1 + t_2. \tag{13}$$

For the adopted hopping parameters, we have $t_C = 0.67t_1$. The band structure for this situation is shown in Fig. 3c.

Now we turn to the edge band crossing. The crossing happens at $k_x = 0$ but nonzero k_y, so we have

$$H_{\text{semi}} = (t_1 + t_2 e^{ik_y d_y}) \begin{bmatrix} 0 & 1 \\ 1 & 0 \end{bmatrix}. \tag{14}$$

Inserting H_{semi} into Eq. (4), we obtain H_{dimer2} under the constriction $k_x = 0$. The eigen values of H_{dimer2} must be zero when the crossing occurs. To ensure this, the value of t_0 has to be

$$t_X = t_2 \left(\frac{t_1}{t_2} + e^{-\kappa d_y} \right)^{-1}, \tag{15}$$

where $\kappa = |k_y|$ is the rate of the edge state decaying to the bulk. By setting $E = 0$ in Eq. (2), we have $\cosh(\kappa d_y) = -t_1/2t_2$, and so the the decay rate is obtained. For our parameters, we have $t_X = 0.12t_1$. The band crossing can be found in Fig. 3d.

In the above discussions, all non-nearest hoppings are neglected. Among them, t_3 has most notable effect

on the edge bands. A nonzero t_3 introduces identical diagonal elements as $4t_3 \cos k_x d_x \cos k_y d_y$ in the bulk Hamiltonian in Eq. (1), which breaks the electron-hole symmetry and induces distortion of edge band curves as well. The bulk band of the ribbons around Γ point is thus lifted by $4t_3 = -0.11t_1$. Because the surrounding situation of the relaxed sites is different from that of bulk ones, the lift of the edge bands is less than the bulk dispersion. This leads to vertically relative displacement between the bulk and edge bands, and make it possible that the edge bands enter the bulk band region without losing the edge property (decay into the bulk), which were verified numerically.

IV. Summary. We studied the edge bands of phosphorene ribbon with relaxed edges by the tight-binding model. The relaxation was modeled by letting the outmost bonds relaxed from the bulk ones. We found there is a critical value of the relaxed hopping for the existence of edge bands within the energy gap, and the value of relaxed hopping for the transition was calculated analytically.

This work was supported by NSF of China Grants # 11274124, 11474106, and 11174088.

1. K. S. Novoselov, A. Geim, S. Morozov, D. Jiang, Y. Zhang, S. Dubonos, I. Grigorieva, and A. Firsov, Science **306**, 666 (2004).
2. A. H. Castro Neto, F. Guinea, N. M. R. Peres, K. S. Novoselov, and A. K. Geim, Rev. Mod. Phys. **81**, 109 (2009).
3. K. F. Mak, C. Lee, J. Hone, J. Shan, and T. F. Heinz, Phys. Rev. Lett. **105**, 136805 (2010).
4. A. Kara, H. Enriquez, A. P. Seitsonen, L. C. L. Y. Voon, S. Vizzini, B. Aufray, and H. Oughaddou, Surf. Sci. Rep. **67**, 1 (2012).
5. F. Xia, H. Wang, and Y. Jia, Nat. Commun. **5**, 4458 (2014).
6. J. D. Wood, S. A. Wells, D. Jariwala, K.-S. Chen, E. Cho, V. K. Sangwan, X. Liu, L. J. Lauhon, T. J. Marks, and M. C. Hersam, Nano Lett. **14**, 6964 (2014).
7. G. Wang, R. Pandey, and S. P. Karna, Nanoscale. **7**, 524 (2014).
8. L. Li, Y. Yu, G. Ye, Q. Ge, X. Ou, H. Wu, D. Feng, X. Chen, and Y. Zhang, Nat. Nanotech. **9**, 372 (2014).
9. T. Low, R. Roldán, H. Wang, F. Xia, P. Avouris, L. M. Moreno, and F. Guinea, Phys. Rev. Lett. **113**, 106802 (2014).
10. A. S. Rodin, A. Carvalho, and A. H. C. Neto, Phys. Rev. B **90**, 075429 (2014).
11. J. Guan, Z. Zhu, and D. Tománek, Phys. Rev. Lett. **113**, 226801 (2014).
12. Q. Wei and X. Peng, Appl. Phys. Lett. **104**, 251915 (2014).
13. A. S. Rodin, A. Carvalho, and A. H. C. Neto, Phys. Rev. Lett. **112**, 176801 (2014).
14. V. Tran, R. Soklaski, Y. Liang, and L. Yang, Phys. Rev. B **89**, 235319 (2014).
15. D. Çakır, H. Sahin, and F. M. Peeters, Phys. Rev. B **90**, 205421 (2014).
16. A. N. Rudenko and M. I. Katsnelson, Phys. Rev. B **89**, 201408(R) (2014).
17. E. T. Sisakht, M. H. Zare, and F. Fazileh, Phys. Rev. B **91**, 085409 (2015).
18. M. Ezawa, New J. Phys. **16**, 115004 (2014).
19. J. Zhang, H. J. Liu, L. Cheng, J. Wei, J. H. Liang, D. D. Fan, J. Shi, X. F. Tang, and Q. J. Zhang, Sci. Rep. **4**, 6452 (2014).
20. H. Guo, N. Lu, J. Dai, X. Wu, and X. C. Zeng, J. Phys. Chem. C **118**, 14051 (2014).
21. Z. Zhu, C. Li, W. Yu, D. Chang, Q. Sun, and Y. Jia, Appl. Phys. Lett. **105**, 113105 (2014).
22. A. Carvalho, A. S. Rodin, and A. H. C. Neto, Europhys. Lett. **108**, 47005 (2014).
23. X. Peng, A. Copple, and Q. Wei, J. Appl. Phys. **116**, 144301 (2014).
24. A. Maity, A. Singh, and P. Sen, arXiv:1404.2469.